Listeria monocytogenes exploits host exocytosis to promote cell-to-cell spread

Georgina C. Dowd[a], Roman Mortuza[a], Manmeet Bhalla[a], Hoan Van Ngo[a], Yang Li[a], Luciano A. Rigano[a], and Keith Ireton[a,1]

[a]Department of Microbiology and Immunology, University of Otago, 9054 Dunedin, New Zealand

Edited by Daniel A. Portnoy, University of California, Berkeley, CA, and approved January 10, 2020 (received for review September 26, 2019)

The facultative intracellular pathogen *Listeria monocytogenes* uses an actin-based motility process to spread within human tissues. Filamentous actin from the human cell forms a tail behind bacteria, propelling microbes through the cytoplasm. Motile bacteria remodel the host plasma membrane into protrusions that are internalized by neighboring cells. A critical unresolved question is whether generation of protrusions by *Listeria* involves stimulation of host processes apart from actin polymerization. Here we demonstrate that efficient protrusion formation in polarized epithelial cells involves bacterial subversion of host exocytosis. Confocal microscopy imaging indicated that exocytosis is up-regulated in protrusions of *Listeria* in a manner that depends on the host exocyst complex. Depletion of components of the exocyst complex by RNA interference inhibited the formation of *Listeria* protrusions and subsequent cell-to-cell spread of bacteria. Additional genetic studies indicated important roles for the exocyst regulators Rab8 and Rab11 in bacterial protrusion formation and spread. The secreted *Listeria* virulence factor InlC associated with the exocyst component Exo70 and mediated the recruitment of Exo70 to bacterial protrusions. Depletion of exocyst proteins reduced the length of *Listeria* protrusions, suggesting that the exocyst complex promotes protrusion elongation. Collectively, these results demonstrate that *Listeria* exploits host exocytosis to stimulate intercellular spread of bacteria.

Listeria | spread | protrusions | exocytosis | exocyst complex

Several intracellular bacterial pathogens, including *Listeria monocytogenes*, *Shigella flexneri*, and *Rickettsia* spp. use an actin-based motility process to spread from infected human cells to neighboring healthy cells (1, 2). After internalization into host cells, bacteria in phagosomes escape to the cytosol. Cytoplasmic microbes stimulate the polymerization of host actin filaments on one bacterial pole, resulting in the formation of actin "comet" tails. These tails propel bacteria through the cytosol and allow contact with the host plasma membrane. Bacteria deform the plasma membrane into protrusions, which are resolved into double-membrane vacuoles that are internalized by neighboring host cells. These vacuoles lyse, releasing bacteria into the cytoplasm and allowing another cycle of spread.

Much progress has been made in understanding the mechanisms of actin polymerization stimulated by *Listeria* or other bacteria that exhibit actin-based motility (1, 2). In the case of *Listeria*, the bacterial surface protein ActA induces the formation of actin filaments by activating the host Arp2/3 complex. Apart from this complex, cofilin and capping proteins play critical roles in actin-based movement by increasing treadmilling of uncapped filaments (3). In contrast to our detailed knowledge of actin-based motility, the mechanism of protrusion formation during cell-to-cell spread is not well understood. Early studies indicated that force generated by actin-based motility contributes to the generation of bacterial protrusions (4). However, it remains unclear whether host processes apart from actin polymerization are exploited by *Listeria* or other bacteria in order to remodel the plasma membrane to generate protrusions.

One process that is known to reshape the plasma membrane to form protrusive structures is polarized exocytosis: the fusion of intracellular vesicles with specific sites in the plasmalemma (5–7). Many polarized exocytic events are spatially controlled by the exocyst, an eight-protein complex that tethers vesicles to sites in the plasma membrane prior to vesicle-plasma membrane fusion mediated by SNARE proteins (6, 7). An intracellular compartment termed the recycling endosome (RE) serves as a source of vesicles for polarized exocytosis controlled by the exocyst (8–10). VAMP3, a v-SNARE protein in the RE, mediates the fusion of RE-derived vesicles with the plasma membrane (6, 11).

The exocyst complex is activated by several GTPases, including Rab8 and Rab11 (6, 7). Importantly, the exocyst and its GTPase regulators promote the formation of plasma membrane protrusions during several biological events, including ciliogenesis, neurite branching, cell migration, phagocytosis, and tunneling nanotube formation (7, 8, 12–15). How the exocyst helps generate protrusive structures is not known, but it is thought to involve localized expansion of the plasma membrane through exocytosis and/or the vesicular transport of proteins that contribute to protrusion formation (7).

In this work, we provide evidence that the efficient generation of protrusions that mediate cell-to-cell spread of *Listeria* requires polarized exocytosis directed by the RE and the exocyst complex. Using an exocytic probe derived from the RE-localized v-SNARE VAMP3, we demonstrate that exocytosis is stimulated in protrusions of *Listeria*. Genetic studies involving RNA interference (RNAi) or dominant negative proteins indicate that exocytosis in protrusions requires the exocyst complex and its regulators Rab8 and Rab11. Further genetic experiments demonstrate important roles for the exocyst complex, Rab8, Rab11, and VAMP3 in

Significance

Whether protrusion formation during cell-to-cell spread of the bacterium *Listeria monocytogenes* involves exploitation of host physiological processes apart from actin polymerization is not understood. In this work, we demonstrate that *Listeria* stimulates the host process of exocytosis in order to efficiently generate protrusions. This stimulation of exocytosis is mediated by the *Listeria* protein InlC and the host exocyst complex. InlC and the exocyst complex control the length of *Listeria* protrusions, suggesting that they regulate protrusion elongation. Our results identify exocytosis as a host process controlling bacterial cell-to-cell spread.

Author contributions: G.C.D., R.M., and K.I. designed research; G.C.D., R.M., M.B., H.V.N., and Y.L. performed research; H.V.N. and L.A.R. contributed new reagents/analytic tools; G.C.D., R.M., Y.L., and K.I. analyzed data; and K.I. wrote the paper.

The authors declare no competing interest.

This article is a PNAS Direct Submission.

Data deposition: All primary data (i.e., raw images of Western blots and Prism files with quantified data) have been deposited in Zenodo, https://zenodo.org/deposit/3614677.

[1]To whom correspondence may be addressed. Email: keith.ireton@otago.ac.nz.

This article contains supporting information online at https://www.pnas.org/lookup/suppl/doi:10.1073/pnas.1916676117/-/DCSupplemental.

First published February 3, 2020.

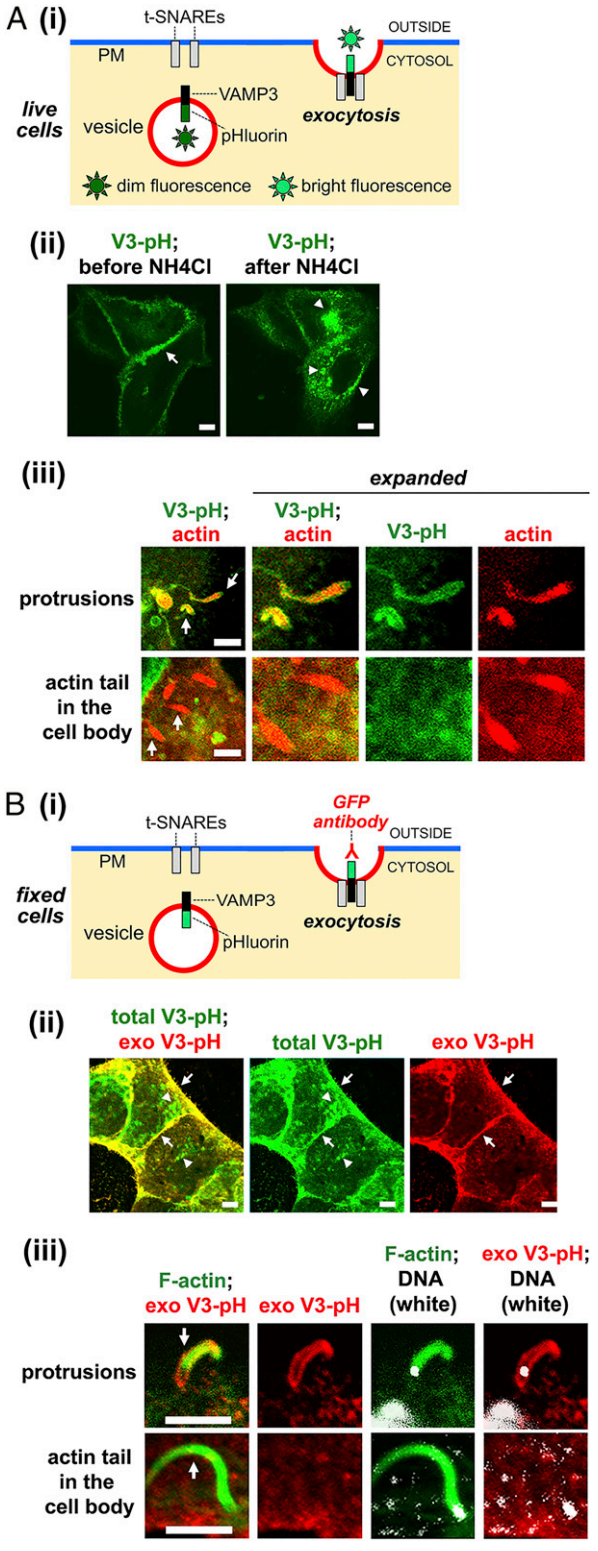

Fig. 1. Exocytosis occurs in *Listeria* protrusions. (*A*) Imaging of exocytosis in live cells. (*i*) Diagram illustrating detection of exocytosis. Superecliptic pHluorin fluoresces brightly at neutral or higher pH, but exhibits dim fluorescence at a pH less than 6.0, typical of endocytic vesicles (28). When fused to the luminal domain of vesicular proteins such as VAMP3, pHluorin becomes brightly fluorescent in live cells upon exposure to the external environment during exocytosis (28–34). (*ii*) Live imaging of VAMP3-pHluorin in uninfected cells. Caco-2 BBE1 cells expressing VAMP3-pHluorin (V3-pH) were imaged before and after addition of 50 mM ammonium chloride (NH_4Cl) for 5 min. The arrow in the *Left* image indicates VAMP3-pHluorin fluorescence at the plasma membrane. The arrowheads in the *Right* image indicate VAMP3-pHluorin fluorescence in intracellular vesicles. (*iii*) Live imaging in infected Caco-2 BBE1 cells. Subconfluent cells stably expressing VAMP3-pHluorin were transiently transfected with a plasmid expressing LifeAct-RFP and infected with WT *Listeria* for 1.5 h in the absence of gentamicin and another 4.5 h in the presence of gentamicin. Imaging of VAMP3-pHluorin (V3-pH) (green) and actin (red) was performed at 37 °C using laser-scanning confocal microscopy. Arrows indicate *Listeria* protrusions or actin comet tails in the cell body. The image on the *Left* is enlarged in panels on the *Right*. (*B*) Imaging of exocytosis in fixed cells. (*i*) Diagram showing detection of exocytosis. When vesicles containing VAMP3-pHluorin fuse with the plasma membrane, exocytosed (exofacial) VAMP3-pHluorin can be detected by labeling with anti-GFP antibodies in the absence of membrane-permeabilizing detergents. (*ii*) Imaging of VAMP3-pHluorin in uninfected fixed cells. Total cellular VAMP3-pHluorin (V3-pH), detected as intrinsic GFP fluorescence, is green. Exofacial VAMP3-pHluorin (exoV3-pH) detected by anti-GFP labeling is red. The *Left* is a merged image, the *Middle* image shows fluorescence of only total V3-pH, and the *Right* image displays fluorescence of only exo V3-pH. The total exoV3 signal is present in both endomembrane compartments (arrowheads) and peripheral areas that represent the plasma membrane (arrows). By contrast, the exo V3-pH is only at the plasma membrane (arrows). (*iii*) Imaging of VAMP3-pHluorin in infected cells. Caco-2 BBE1 cells expressing VAMP3-pHluorin were infected with WT *Listeria* for 1.5 h in the absence of gentamicin and another 4.5 h in the presence of gentamicin. Cells were then fixed and labeled for exofacial VAMP3-pHluorin [exo V3-pH (red), filamentous actin (green), and DNA (white)] as described in *Materials and Methods*. Arrows indicate a *Listeria* protrusion or actin comet tail in the cell body. The white body at the tip of the protrusion or comet tail is a bacterium. (Scale bars, 5 μm.)

protrusion formation and cell-to-cell spread by *Listeria*. Measurement of protrusion lengths indicates that the exocyst complex controls the growth of *Listeria* protrusions.

Results

Exocytosis Is Up-Regulated in Protrusions of *Listeria*. *L. monocytogenes* is a food-borne pathogen (16, 17), and infection of the intestinal epithelium is the first step in listeriosis (18, 19). We used the human enterocyte cell line Caco-2 BBE1 to investigate if exocytosis occurs in protrusions made by *Listeria*. This cell line has the ability to polarize in cell culture, producing a monolayer that has similarities to the intestinal cell barrier (20). Importantly, Caco-2 BBE1 cells or other polarized epithelial cells have been extensively used to investigate mechanisms of cell-to-cell spread of *Listeria* (21–26).

In order to detect exocytosis in Caco-2 BBE1 cells, we constructed an exocytic probe consisting of the v-SNARE protein VAMP3 fused to pHluorin, a pH-sensitive form of GFP (27, 28). This GFP variant has been widely used to image exocytosis in live cells (29–34) (Fig. 1 *A*, *i*). The VAMP3-pHluorin construct can also be used to detect exocytosis in fixed cells by labeling with anti-GFP antibodies in the absence of plasma membrane permeabilization (8) (Fig. 1 *B*, *i*). Two control experiments indicated that the VAMP3-pHluorin probe detected exocytosis. First, live-cell imaging detected bright GFP fluorescence primarily at the plasma membrane of cells (Fig. 1 *A*, *ii*). Incubation of cells with ammonium chloride, which is known to neutralize the pH of endosomes, induced fluorescence in intracellular vesicles. Second, incubation of fixed, nonpermeabilized cells with an antibody against GFP resulted in labeling of VAMP3-pHluorin at the plasma membrane, but not in endosomes (Fig. 1 *B*, *ii*).

The VAMP3-pHluorin probe was used to determine if exocytosis occurs in protrusions of *Listeria*. Initial experiments were performed with subconfluent Caco-2 BBE1 cells in order to readily detect protrusions as structures containing actin comet tails that project into empty space. In live-imaging studies involving cells expressing VAMP3-pHluorin and LifeAct-RFP (35) to label comet tails, exocytosis was detected in protrusions of the wild-type (WT) *Listeria* strain EGD (Fig. 1 *A*, *iii*). Importantly, actin comet

tails in the cell body exhibited little or no fluorescence of VAMP3-pHluorin. Similarly, work with fixed cells demonstrated labeling of exocytosed (exofacial) VAMP3-pHluorin in protrusions of *Listeria*, but not in comet tails in the cell body (Fig. 1 *B*, *iii*).

Next, we examined if exocytosis is enhanced in *Listeria* protrusions compared to other areas of the host plasma membrane by determining fold enrichment (FE) values. FE is defined as "the mean pixel intensity of exofacial VAMP3-pHluorin in protrusions compared to the mean pixel intensity throughout the entire plasma membrane of the host cell." An FE value greater than 1.0 indicates enrichment of the exocytosed probe in protrusions. Subconfluent Caco-2 BBE1 cells stably expressing VAMP3-pHluorin were used for these studies (Fig. 2 *A*, *i*). An analysis of ∼150 protrusions made by WT *Listeria* in fixed cells revealed an average FE of 2.1 (Fig. 2 *A*, *ii*). These results indicate a two-fold enhancement in exocytosis at protrusions of WT *Listeria*, suggesting that bacteria stimulate exocytosis. Since efficient formation of *Listeria* protrusions in Caco-2 BBE1 cells requires the secreted bacterial virulence factor InlC (22–25), we investigated if InlC contributes to exocytosis. (Fig. 2 *A*, *i*). The mean FE value for protrusions of a bacterial mutant deleted for the *inlC* gene (Δ*inlC*) (22) was 1.1, ∼50% of that of protrusions of WT *Listeria* (Fig. 2 *A*, *ii*). These findings demonstrate that InlC contributes to exocytosis in protrusions.

Although *Listeria* makes protrusions in subconfluent cells, it cannot efficiently spread in such conditions because of a lack of neighboring host cells available to internalize protrusions. We therefore assessed exocytosis in protrusions of confluent, polarized Caco-2 BBE1 cells grown in transwell devices. In confluent monolayers, *Listeria* protrusions project into neighboring host cells and cannot be readily distinguished from actin tails in the cell body of an adjacent cell by simply labeling F-actin. We therefore developed an approach involving generating a population of human cells with a marker capable of detecting protrusions and mixing this population with an excess of unlabeled host cells. After infection, protrusions are detected as bacterial-associated F-actin structures projecting from labeled host cells into unlabeled cells. We used the intrinsic GFP fluorescence of VAMP3-pHluorin (blue in Fig. 2 *B*, *i*) to mark protrusions in fixed cells. Caco-2 BBE1 cells stably expressing VAMP3-pHluorin were mixed with normal Caco-2 BBE1 cells at a 1:3 ratio, followed by infection with *Listeria*, fixation, and labeling for exofacial VAMP3-pHluorin. Similar to the situation in subconfluent cells, exocytosed VAMP3-pHluorin was detected in protrusions of WT and Δ*inlC* mutant strains of *Listeria* (Fig. 2 *B*, *i*). The average degree of exocytosis in protrusions of the WT bacterial strain was about two-fold higher than that in protrusions of the Δ*inlC* mutant (Fig. 2 *B*, *ii*). These findings demonstrate that InlC enhances exocytosis in protrusions in polarized Caco-2 BBE1 cells.

The Host Exocyst Complex and Its GTPase Regulators Promote Cell-To-Cell Spread of *Listeria*. Because the exocyst complex is known to promote polarized exocytic events (7), we investigated the role of this complex in protrusion formation by *Listeria*. Interestingly, the exocyst component Exo70 (Fig. 3*A*) accumulated in protrusions made by WT *Listeria* (Fig. 3 *B*, *i*). A comparison of FE values for Exo70 in protrusions of WT and Δ*inlC* mutant strains indicated that InlC contributed to recruitment of Exo70 to protrusions (Fig. 3 *B*, *ii*). In addition, coprecipitation experiments

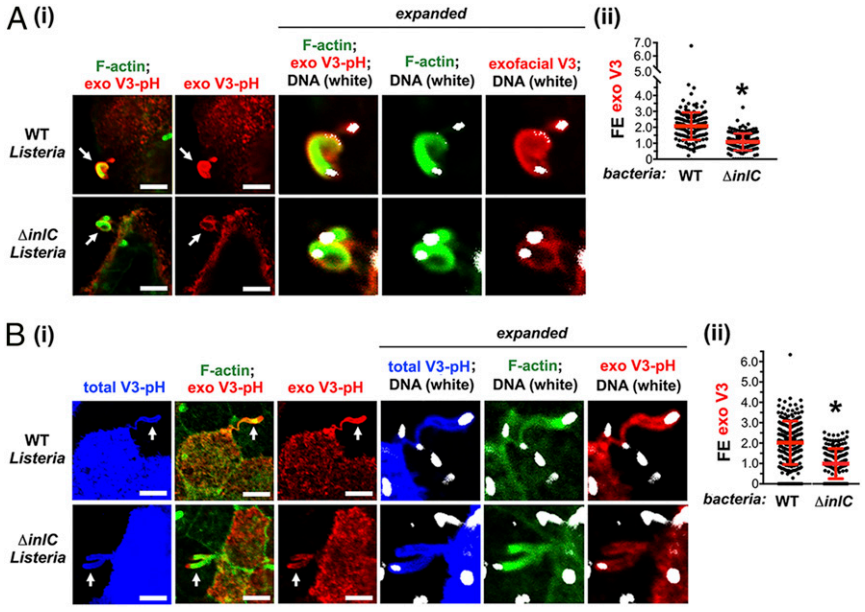

Fig. 2. Exocytosis is up-regulated in *Listeria* protrusions. (*A*) Results in subconfluent Caco-2 BBE1 cells. Cells expressing VAMP3-pHluorin were infected with WT or Δ*inlC* mutant strains of *Listeria* for 1.5 h in the absence of gentamicin and another 4.5 h in the presence of gentamicin, followed by fixation and labeling of exofacial VAMP3-pHluorin [exo V3-pH (red), F-actin (green), or DNA (white)]. (*i*) Representative confocal microscopy images of bacterial protrusions are presented. Protrusions are indicated by arrows, and regions around protrusions are expanded in panels on the *Right*. White objects at the end of protrusions are bacteria. (Scale bars, 5 μm.) (*ii*) FE data for exofacial VAMP3-pHluorin (exo V3) in bacterial protrusions are presented. Each dot represents an FE measurement. Data are mean ± SD of 165 or 166 FE values for WT or Δ*inlC Listeria* strains, respectively. **P* < 0.0001. (*B*) Results in confluent Caco-2 BBE1 cells. Caco-2 BBE1 cells stably expressing VAMP3-pHluorin were mixed with normal Caco-2 BBE1 cells at a ratio of 1:3 and grown to confluency. Cells were infected with WT or Δ*inlC* strains of *Listeria* for 1.5 h in the absence of gentamicin and another 4.5 h in the presence of gentamicin, followed by labeling of exofacial VAMP3-pHluorin [exo V3-pH (red), F-actin (green), and DNA (white)]. Intrinsic GFP fluorescence [total V3-pH (blue)] was used to identify protrusions from cells expressing VAMP3-pHluorin that project into surrounding cells lacking VAMP3-pHluorin. (*i*) Representative confocal microscopy images are shown. Protrusions are indicated with arrows on the *Left*. Regions around protrusions are enlarged in panels on the *Right*. White objects (labeled for DNA) are bacteria. (Scale bars, 5 μm.) (*ii*) FE data for exofacial VAMP3-pHluorin (exo V3) in protrusions are displayed. Each dot indicates an FE measurement. Data are mean ± SD of 151 or 173 FE values for WT or Δ*inlC Listeria* strains, respectively. **P* < 0.0001.

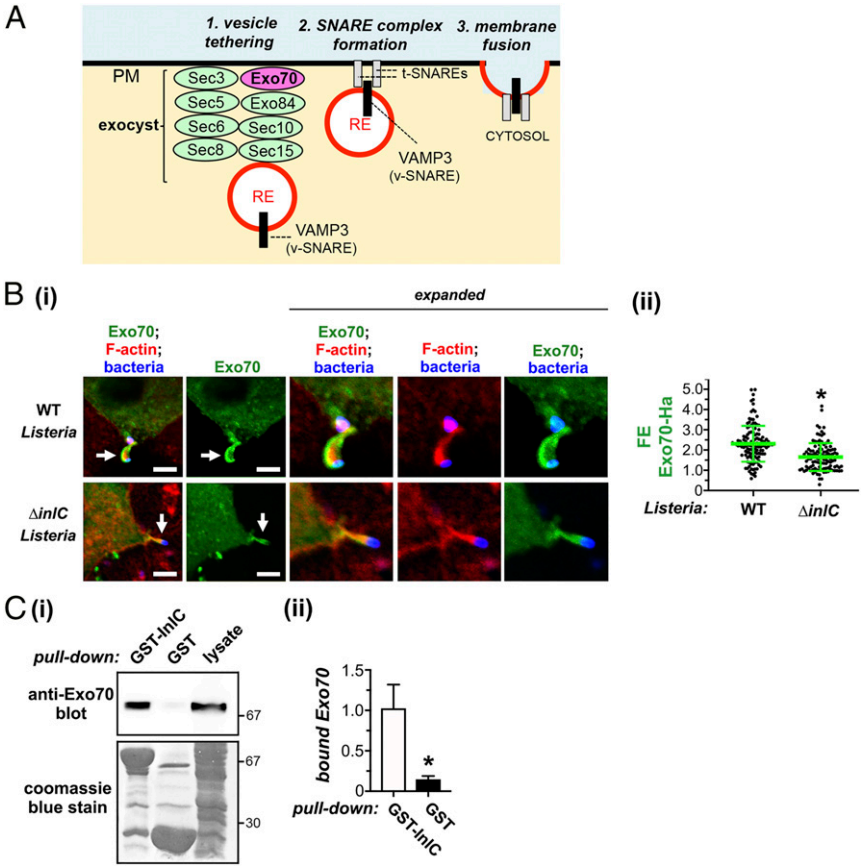

Fig. 3. The *Listeria* protein InlC associates with host Exo70 and recruits Exo70 to protrusions. (*A*) Diagram of the exocyst complex. Exo70 is colored magenta, whereas the remaining seven exocyst components are green. Exo70 interacts with the lipid phosphatidylinositol 4,5-bis phosphate and is thought to anchor the exocyst complex to the plasma membrane (PM) (7, 36). The exocyst tethers vesicles derived from the RE to the plasma membrane prior to fusion mediated by SNARE proteins. (*B*) InlC-dependent recruitment of Exo70 to protrusions. Caco-2 BBE1 cells were transiently transfected with a plasmid expressing Ha-tagged Exo70 and then infected with WT or Δ*inlC* strains of *Listeria* for 6 h. Cells were then fixed and labeled for Exo70-Ha (green), F-actin (red), or *Listeria* (blue). (*i*) Representative images are shown. Transient transfection typically results in ∼25% of the Caco-2 BBE1 cell population expressing Exo70-Ha. Arrows in *Left* panels indicate protrusions from cells expressing Exo70-Ha that project into nearby cells lacking Exo70-Ha. Regions with protrusions are expanded in panels on the *Right*. (Scale bars indicate 5 μm.) (*ii*) FE data for Exo70-Ha in protrusions are presented. Each dot represents an FE measurement. Data are mean ± SD of 129 or 110 FE values for WT or Δ*inlC Listeria* strains, respectively. $*P < 0.0001$. (*C*) Association of InlC with Exo70. Lysates of Caco-2 BBE1 cells were used for coprecipitation experiments with a purified fusion protein consisting of GST fused to InlC (GST-InlC) or with GST alone. Following precipitation and washing of GST-tagged proteins, Exo70 in precipitates was detected by Western blotting. (*i*) A Western blotting image from a representative experiment is shown. (*Top*) An anti-Exo70 Western blot of precipitates. (*Bottom*) The membrane used for the anti-Exo70 Western blot was stripped and stained with Coomassie blue in order to confirm precipitation of GST-InlC (∼67 kDa) or GST (∼29 kDa). (*ii*) Quantified Western blotting data of Exo70 association are presented. Data are mean levels of bound Exo70 ± SEM from five experiments. $*P = 0.018$.

using a GST-InlC fusion protein demonstrated that Exo70 associates with InlC (Fig. 3*C*).

We then used RNAi to assess the role of the exocyst complex and also the v-SNARE VAMP3 in bacterial protrusion formation and spread. Small interfering RNAs (siRNAs) were used to deplete VAMP3 or the exocyst components Exo70, Sec5, or Sec8 in confluent Caco-2 BBE1 cells, and the resulting effect on bacterial protrusions was assessed. Protrusions were quantified using a previously described approach that detects protrusions labeled with enhanced green fluorescent protein (EGFP)-actin projecting into nearby host cells lacking EGFP-actin (*SI Appendix*, Fig. S1) (22–25). Importantly, depletion of the various exocyst components or VAMP3 caused a 30 to 50% reduction in the formation of protrusions by WT *Listeria* (Fig. 4). Interestingly, knockdown of Exo70, Sec5, Sec8, or VAMP3 did not further reduce residual protrusion formation by Δ*inlC* mutant bacteria. These latter findings indicate that the exocyst and VAMP3 control InlC-mediated spread and do not play a detectable role in low-level spread occurring in the absence of InlC. Importantly, depletion of the exocyst components or VAMP3 did not affect the proportion of WT or Δ*inlC* bacteria that recruited F-actin or the length of F-actin comet tails (*SI Appendix*, Fig. S2). These results indicate that the exocyst and VAMP3 do not control actin-based motility and therefore likely directly affect protrusion formation.

The exocyst complex is positively regulated by several GTPases, including Rab11A and Rab8A (7, 36). Expression of EGFP- or cyan fluorescent protein (CFP)-tagged dominant negative forms of Rab11A (Rab11A.S25N) or Rab8A (Rab8A.T22N) inhibited protrusion formation by WT *Listeria* without affecting bacterial association with F-actin or actin comet tail length (Fig. 5*A* and *SI Appendix*, Fig. S3). These findings support the results in Fig. 4, providing further evidence that the exocyst complex promotes the generation of bacterial protrusions.

Since protrusions mediate cell-to-cell spread of *Listeria* (1, 2), we used a previously described microscopy-based approach to determine if the exocyst complex or Rab proteins are needed for bacterial spread. This method involves measuring the surface area of foci of infection in monolayers of Caco-2 BBE1 cells (23–25). Importantly RNAi-mediated depletion of Sec5 reduced the

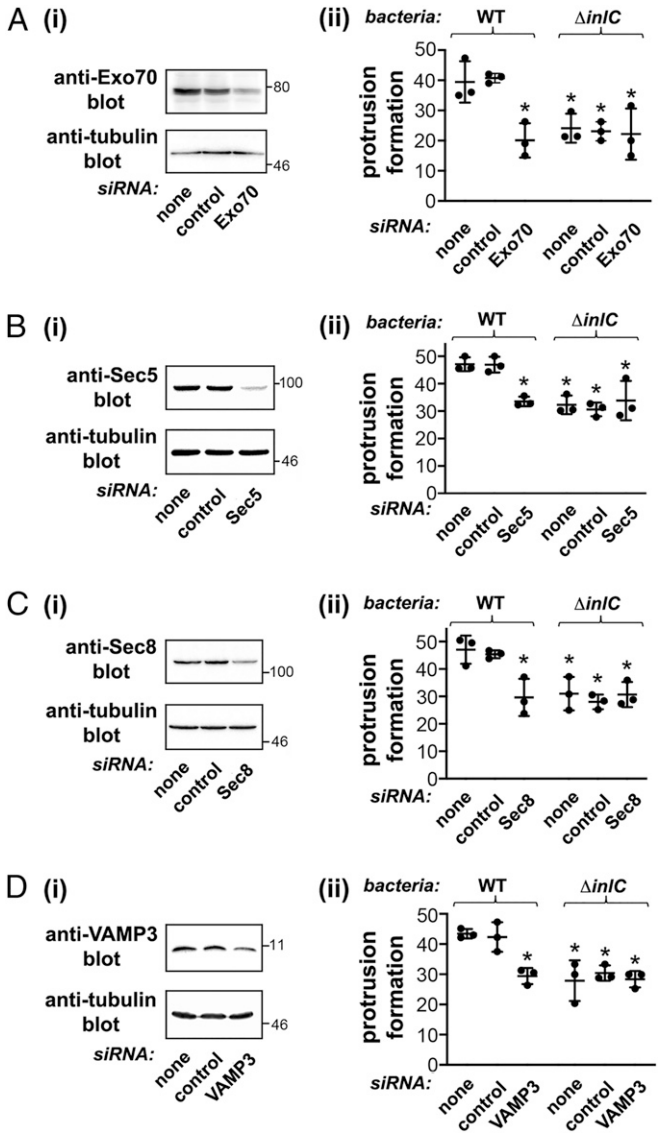

Fig. 4. The host exocyst complex and the SNARE protein VAMP3 promote the formation of *Listeria* protrusions. Caco-2 BBE1 cells were either mock-transfected in the absence of siRNA, transfected with a control nontargeting siRNA, or transfected with siRNAs targeting Exo70 (*A*), Sec5 (*B*), Sec8 (*C*), or VAMP3 (*D*). Cells were then transfected with a plasmid expressing EGFP-actin. About 48 h after plasmid DNA transfection, cells were either solubilized for confirmation of depletion of target proteins by Western blotting (*i*) or infected with WT or Δ*inlC* strains of *Listeria* for 6 h to assess protrusion formation efficiency. (*ii*) Approximately 25% of the Caco-2 BBE1 cell population expressed EGFP-actin. Protrusions were identified as structures containing EGFP-actin and bacteria that projected into surrounding cells lacking EGFP-actin expression. Protrusion efficiency was quantified as described in *SI Appendix, SI Materials and Methods*. Each dot represents a mean protrusion efficiency value from a single experiment. Horizontal bars denote the average protrusion efficiency from three experiments. Error bars are SD. **P* < 0.05 compared to the mock transfection or control siRNA conditions for the WT *Listeria* strain.

size of foci produced by WT *Listeria*, indicating a role for the exocyst in cell-to-cell spread (Fig. 5 *B*, *i*, and *SI Appendix*, Fig. S4). In Caco-2 BBE1 cells stably expressing EGFP-tagged Rab11A.S25N or CFP-tagged Rab8A.T22N proteins, foci made by WT *Listeria* were smaller than foci produced in control cells expressing EGFP alone (Fig. 5 *B*, *ii* and *iii*, and *SI Appendix*, Fig. S5). Collectively, the findings in Fig. 5*B* and *SI Appendix*, Figs. S4 and S5, demonstrate an important role for the exocyst and its regulators in the intercellular spread of *Listeria*.

The Exocyst Complex Mediates Exocytosis in Bacterial Protrusions. The simplest interpretation of the data presented thus far is that the exocyst complex contributes to *Listeria* protrusion formation by stimulating exocytosis in protrusions. In order to directly test this idea, RNAi was used to deplete Exo70 or Sec5 in confluent Caco-2 BBE1 cells stably expressing VAMP3-pHluorin. Exocytosis was quantified as FE values for exofacial VAMP3-pHluorin. Importantly, depletion of Exo70 or Sec5 reduced exocytosis in protrusions of WT *Listeria*, but not in protrusions made by the

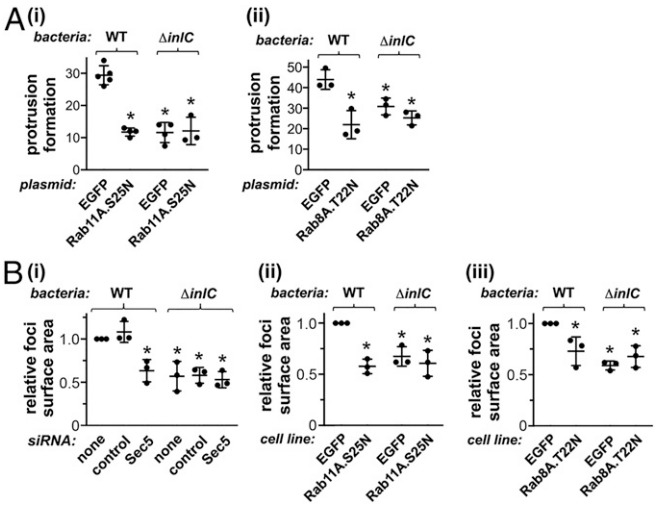

Fig. 5. The exocyst protein Sec5 and the host GTPases Rab11 and Rab8 control cell-to-cell spread of *Listeria*. (*A*) Rab11 and Rab8 promote bacterial protrusion formation. Caco-2 BBE1 cells were transiently transfected with plasmids expressing EGFP alone, EGFP-tagged dominant negative Rab11A (Rab11A.S25N), or CFP-tagged dominant negative Rab8A (Rab8A.T22N). Cells were then infected with WT or Δ*inlC* strains of *Listeria* for 1.5 h in the absence of gentamicin and another 4.5 h in the presence of gentamicin. Cells were then fixed, labeled, and imaged by confocal microscopy, as described in *Materials and Methods*. Approximately 25% of transfected Caco-2 BBE1 cells expressed the EGFP or CFP-tagged proteins. Protrusions were identified as structures with F-actin comet tails and bacteria that projected from EGFP- or CFP-positive cells into surrounding cells that lacked EGFP- or CFP-tagged proteins. (*i*) Inhibition of protrusion formation by Rab11A.S25N. Protrusion formation data are means ± SD from three to five experiments, depending on the condition. Each dot represents a protrusion efficiency value from a single experiment. **P* < 0.05 compared to the EGFP control with the WT *Listeria* strain. (*ii*) Reduction in protrusion formation by Rab8A.T22N. Data are means ± SD from three experiments. **P* < 0.05 compared to EGFP control with the WT *Listeria* strain. (*B*) Sec5, Rab11, and Rab8 promote cell-to-cell spread. (*i*) Role of Sec5 in spread. Caco-2 BBE1 cells were mock-transfected in the absence of siRNA, transfected with a control siRNA, or transfected with an siRNA against Sec5. Cells were then infected with WT or Δ*inlC* strains of *Listeria* for 1.5 h in the absence of gentamicin and 10.5 h in the presence of gentamicin, followed by labeling of bacteria and F-actin to detect cell borders. (*ii*) Contribution of Rab11 to cell-to-cell spread. Caco-2 BBE1 cells stably expressing EGFP or EGFP-tagged Rab11A.S25N were infected with the indicated *Listeria* strains for 1.5 h in the absence of gentamicin followed by 10.5 h in the presence of gentamicin. Cells were then fixed and labeled for *Listeria* and F-actin. (*iii*) Role of Rab8A in spread. Caco-2 BBE1 cells stably expressing EGFP alone or CFP-tagged Rab8A.T22N were infected with the indicated *Listeria* strains, followed by fixation and labeling. Samples in *i*, *ii*, and *iii* were imaged by confocal microscopy, and surface areas of infection foci were measured using Image J software. Data in *B* are mean relative foci size ± SD from three experiments. Each dot represents the average focal size in a single experiment. In each experiment, ~25 foci were measured for each condition. **P* < 0.05 compared to the mock transfection or control siRNA conditions (*i*) or the EGFP condition (*ii* and *iii*) in the WT *Listeria* strain.

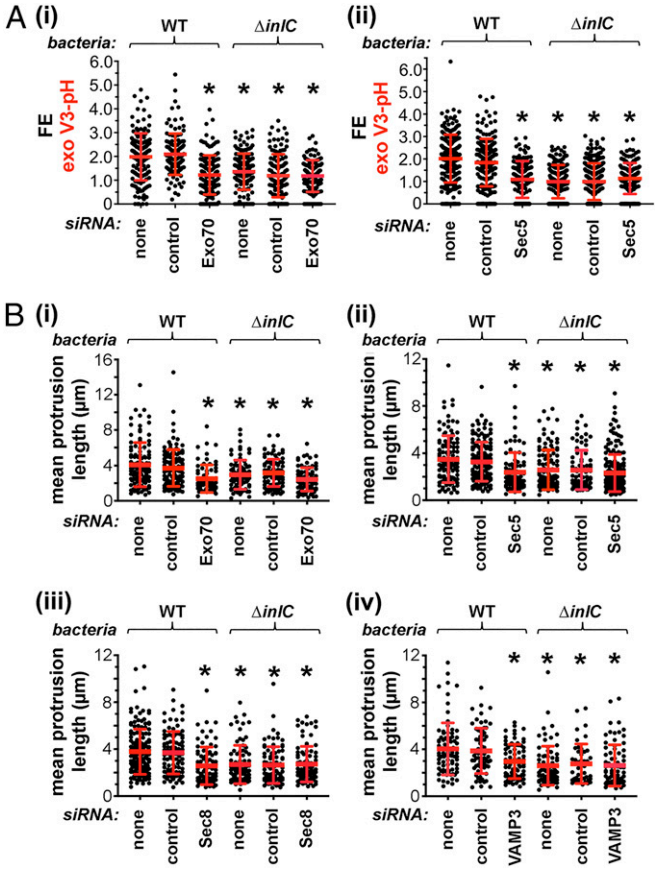

Fig. 6. The exocyst complex mediates exocytosis in *Listeria* protrusions and controls protrusion lengths. (*A*) Role of the exocyst in exocytosis in protrusions. Caco-2 BBE1 cells stably expressing VAMP3-pHluorin condition were mixed with normal Caco-2 BBE1 cells at a 1:3 ratio. Cells were then mock-transfected in the absence of siRNA, transfected with a control siRNA, or transfected with siRNAs targeting Exo70 (*i*) or Sec5 (*ii*). After transfection, cells were infected with WT or Δ*inlC* strains of *Listeria* for 1.5 h in the absence of gentamicin and another 4.5 h in the presence of gentamicin. Cells were then fixed and labeled for exofacial VAMP3-pHluorin (exo V3-pH), F-actin, and bacteria. Samples were imaged by confocal microscopy, and ImageJ software was used to quantify FE values for exo V3-pH. Each dot in the graphs indicates an FE measurement. Data in *i* and *ii* are means ± SD of 115 to 249 FE values, depending on the condition. *$P < 0.005$. (*B*) Role of the exocyst complex and VAMP3 in controlling lengths of protrusions. Caco-2 BBE1 cells were mock-transfected in the absence of siRNA, transfected with a control siRNA, or transfected with siRNAs targeting Exo70 (*i*) or Sec5 (*ii*), Sec8 (*iii*), or VAMP3 (*iv*). Cells were then transiently transfected with a plasmid expressing EGFP-actin in order to allow detection of protrusions and then infected for 1.5 h in the absence of gentamicin and another 4.5 h in the presence of gentamicin with WT or Δ*inlC* strains of *Listeria*. Cells were fixed and labeled for F-actin and bacteria. Samples were imaged by confocal microscopy, and ImageJ software was used to measure lengths of protrusions. The lengths of ∼120 actin tails were measured for each condition. *$P < 0.005$.

Δ*inlC* mutant strain (Fig. 6*A* and *SI Appendix*, Fig. S6). This effect of Exo70 or Sec5 depletion on exocytosis was genuine and was not an artifact due to altered expression of VAMP3-pHluorin (*SI Appendix*, Fig. S7). In combination with the findings in Figs. 3 to 5, the results in Fig. 6*A* demonstrate that the exocyst complex contributes both to exocytosis in protrusions and to the generation of protrusions. It therefore seems likely that the exocyst controls protrusion formation through its effects on exocytosis.

The Exocyst Complex Controls the Length of Protrusions. RNAi-mediated depletion of exocyst proteins or VAMP3 reduced the formation of *Listeria* protrusions, but did not abolish the production of these structures (Fig. 4). We used ImageJ software to measure the lengths of protrusions made by WT or Δ*inlC* mutant bacteria in cells subjected to control conditions or depleted for Exo70, Sec5, Sec8, or VAMP3. Knockdown of exocyst proteins or VAMP3 reduced the mean lengths of protrusions made by WT *Listeria*, but did not affect the lengths of protrusions made by Δ*inlC* mutant bacteria (Fig. 6*B*). These findings suggest that exocytosis may promote the elongation of protrusions of WT *Listeria*.

Discussion

In this work, we report a role for host exocytosis in cell-to-cell spread of *Listeria* in polarized epithelial cells. Several lines of evidence indicate that *Listeria* actively exploits host exocytosis to produce protrusions. First, exocytosis mediated by the RE pathway was up-regulated in protrusions of WT *Listeria*. Second, WT bacteria recruited Exo70 to protrusions. Finally, RNAi-mediated knockdown of exocyst components impaired exocytosis in *Listeria* protrusions, reduced the frequency of protrusion formation, and inhibited cell-to-cell spread of bacteria.

The exocyst holocomplex is composed of eight proteins: Exo70, Exo84, Sec3, Sec5, Sec6, Sec8, Sec10, and Sec15 (36). This holocomplex can be further divided into subcomplexes I (Sec3, Sec5, Sec6, and Sec8) and II (Sec10, Sec15, Exo70, and Exo84). An interesting question is whether particular exocytic pathways in mammalian cells require the exocyst holocomplex or instead are mediated by a specific subcomplex (36). Most of the available data to date suggest an important role for the holocomplex in mediating specific pathways of exocytosis. For example, insulin-induced exocytosis of the GLUT4 receptor requires Sec5, Sec6, Sec8, Sec10, Exo70, and Exo84 (37), indicating involvement of both subcomplexes I and II. We found that RNAi-mediated depletion of Exo70, Sec5, or Sec8 each impairs protrusion formation and spread of *Listeria*. These results suggest that intercellular dissemination of *Listeria* involves exploitation of the exocyst holocomplex. Another salient issue is whether the role of the exocyst in spread of *Listeria* could involve activities apart from exocytosis. Such a scenario seems unlikely for the following reasons. First, RNAi-mediated depletion of Exo70 or Sec5 reduced both exocytosis in *Listeria* protrusions and the formation of these structures, indicating a link between exocytosis and bacterial spread. Second, of the eight exocyst proteins, only Exo70 is known to control a process apart from exocytosis. Exo70 is capable of stimulating actin polymerization through the Arp2/3 complex (38, 39). However, our results demonstrate that depletion of Exo70 fails to affect the formation of actin comet tails by *Listeria*, indicating that this exocyst protein is dispensable for actin-based motility. Collectively, our findings provide compelling evidence that the exocyst complex promotes *Listeria* protrusion formation and spread through its established function in polarized exocytosis.

How does *Listeria* stimulate exocytosis at sites of protrusion formation? At present, the mechanism of regulation of exocytosis during cell-to-cell spread is not well understood. However, our findings that the secreted *Listeria* virulence factor InlC promotes exocytosis in protrusions and associates with Exo70 suggests that InlC may manipulate exocyst function. Interestingly, previous results indicate that InlC controls *Listeria* protrusion formation, at least in part, by binding and antagonizing the human scaffolding protein Tuba (22, 23). During apical lumen formation in epithelia, Tuba acts downstream of the GTPases Rab8A and Rab11A to control exocytosis through the exocyst complex (40). Future work should determine whether Tuba acts as a regulator of the exocyst to affect the generation of *Listeria* protrusions.

An important question is, how does stimulation of exocytosis affect the cell-to-cell spread of *Listeria*? Our results indicate that RNAi-mediated depletion of exocyst components or VAMP3

caused two effects on protrusions made by WT *Listeria*. First, the number of protrusions generated was reduced by 30 to 50%. Second, the lengths of the remaining protrusions decreased by 25 to 30%. Taken together, these findings suggest that host exocytosis may regulate both the initiation and the elongation of protrusions. An alternative interpretation of these data is that exocytosis might affect the stability of protrusions and that these structures collapse more readily when components of the exocyst complex are depleted. Distinguishing between these possible interpretations will require detailed kinetic analysis of protrusion formation in future work.

We present three speculative ideas for how exocytosis might control the initiation or elongation or *Listeria* protrusions. First, exocytosis could translocate host proteins with membrane remodeling activity to the plasma membrane (*SI Appendix*, Fig. S8*A*). Such proteins would associate with the cytoplasmic face of RE-derived vesicles, cycling between these vesicles and the plasmalemma. Precedents for this idea involve the GTPase Dynamin 2 and the signaling protein Cdc42GAP, which are transported from the RE to the plasma membrane through exocytosis (41, 42). Second, exocytosis might control the initiation of *Listeria* protrusion formation through effects on plasma membrane tension (*SI Appendix*, Fig. S8*B*). There is evidence to suggest that exocytosis decreases membrane tension, although the mechanism of this effect remains unclear (43). InlC is known to relieve membrane tension at apical junctions by antagonizing host Tuba protein, thereby facilitating protrusion formation (22, 23). An interesting idea is that Tuba might generate membrane tension by limiting activity of the exocyst. By inhibiting Tuba, InlC would up-regulate exocytosis and relieve tension, thereby allowing bacteria to initiate formation of protrusions. Finally, we propose that polarized exocytosis could potentially promote the elongation of *Listeria* protrusions by delivering host membrane to these structures (*SI Appendix*, Fig. S8*C*). Clearly, future work is needed to test each of these potential mechanisms of regulation of protrusion initiation and elongation.

Our study focuses on exocytic events in the host cell that donates protrusions. It is possible that exocytosis is also locally up-regulated in the plasma membrane of cells that accept (internalize) *Listeria* protrusions. Such coordination of exocytosis in the two host-cell populations could stabilize protrusions that have initiated, promote elongation of protrusions, and/or affect the internalization of these structures. Future work measuring exocytosis and inhibiting exocyst proteins specifically in host cells accepting protrusions should answer whether the spread of *Listeria* requires up-regulation of exocytosis in both host-cell populations.

Until this study, actin polymerization was the only host physiological process known to be exploited by *Listeria* to stimulate the formation of protrusions that mediate cell-to-cell spread (1, 2). Apart from *Listeria*, several other microbes induce the formation of protrusive structures in order to efficiently infect human cells. The intracellular bacterial pathogens *S. flexneri* and *Rickettsia* spp. resemble *Listeria* in using actin-based motility in the host cytosol to produce protrusions that promote spread (1, 2). Similarly to *Listeria*, *Shigella*, or *Rickettsia*, enteropathogenic *Escherichia coli* (EPEC) or vaccinia virus also stimulate actin polymerization and the formation of protrusive structures (44, 45). However, EPEC and vaccinia virus form these protrusive structures (also called "pedestals") on the apical surface of host cells, rather than inside cells. An interesting question is whether host exocytosis has a general role in the formation of protrusions by microbial pathogens. Future studies with *Shigella*, *Rickettsia*, EPEC, and/or vaccinia virus should answer this question.

Finally, we note that exploitation of the host exocyst complex has previously been observed with the bacterium *Salmonella enterica* serovar typhimurium (46). The bacterial protein SipC, present at the tip of a type III secretion system, inserts into the host plasma membrane and interacts with Exo70 in the cytosol. This interaction contributes to plasma membrane ruffling and internalization of *Salmonella* into host cells. Our findings with *Listeria* combined with the previous results with *Salmonella* indicate that the exocyst complex can be targeted to promote different stages in the intracellular life cycle of pathogens, including spread and entry.

Materials and Methods

See *SI Appendix* for additional materials and methods.

Cell Culture and Transfection. The human enterocyte cell line Caco-2 BBE1 (20) or Caco-2 BBE1 cell lines stably expressing VAMP3-pHluorin, GFP-tagged Rab11.S25N, or CFP-tagged Rab8A.T22N were grown on transwell permeable supports (Corning 3450; 0.4-μm pore size) in Dulbecco's Modified Eagle Media (DMEM) supplemented with 10% fetal bovine serum, 10 μg/mL human transferrin, and penicillin/streptomycin at 37 °C in 5% CO_2. For experiments involving RNAi, cells were reversed-transfected in the presence of 100 nM siRNA using Lipofectamine RNAiMax (Thermo Fisher Scientific) according to the manufacturer's instructions. Plasmid DNA transfection was performed using Lipofectamine 2000 (Thermo Fisher Scientific) as previously described (25).

Bacterial Infection. Caco-2 BBE1 cells were incubated in DMEM and infected with the WT *Listeria* strain EGD or with an isogenic strain deleted for the *inlC* gene (Δ*inlC*) (22) using a multiplicity of infection of ∼10:1. Infections for experiments assessing protrusion formation were performed for 1.5 h in the absence of gentamicin and for another 4.5 h in medium with gentamicin. For studies measuring cell-to-cell spread with focus assays, infection was performed for 1.5 h without gentamicin and for 10.5 h with gentamicin.

Western Blotting and Coprecipitation Experiments. Western blotting, quantification of Western blots, and coprecipitation with GST or GST-InlC were carried out using lysates of Caco-2 BBE1 cells as described previously (25).

Confocal Microscopy. For live-imaging work, infected cells in two-chambered slides (μ-slide with 2 wells; Ibidi) were placed in a 37 °C incubator attached to an Olympus FV1200 laser-scanning confocal microscope. Samples were imaged using a 60× 1.30 numerical aperture (NA) silicon oil immersion objective. Laser lines of 488 and 543 nm were used for excitation, and a two-channel GaAsP detector was used for detection of pHluorin and LifeAct-RFP. For imaging of cells fixed with 3% paraformaldehyde (PFA), a 60× 1.35 NA oil immersion objective was used with the FV1200 confocal microscope. Laser lines of 405, 488, 543, and 633 nm were used for excitation, and photomultiplier tube detectors were used for image capture. Images from serial sections spaced 1.0 μm apart were taken to ensure that all *Listeria* protrusions were detected.

Quantification of Protrusion Formation. Caco2-BBE1 cells were transiently transfected with a plasmid expressing EGFP-tagged actin, resulting in about 25% of the cell population expressing the tagged protein. The efficiency of formation of *Listeria* protrusions was measured using a previously described approach that detects protrusions as F-actin tails projecting from cells expressing EGFP-actin into adjacent cells lacking EGFP-actin (22–25).

Measurement of F-Actin Recruitment, Actin Tail Lengths, and Protrusion Lengths. F-actin recruitment efficiencies were quantified as the percentage of total bacteria in the main body of the host cell that were decorated with F-actin, as previously described (22–25). ImageJ software was used to measure the lengths of actin comet tails or protrusions made by *Listeria*, as previously detailed (22–25).

Quantification of Exocytosis or Recruitment of Exo70. For detection of exocytosis in protrusions, Caco-2 BBE1 cells stably expressing VAMP3-pHluorin were mixed with normal Caco-2 cells at a 1:3 ratio. Cells were then infected with WT or Δ*inlC* strains of *Listeria* and fixed in 3% PFA. Labeling of exofacial VAMP3-pHluorin was performed using mouse anti-GFP antibodies (Sigma-Aldrich) on unpermeabilized cells, essentially as described (8). Secondary anti-mouse antibodies coupled to Alexa Fluor 647 were used for detection. Samples were then permeabilized and labeled with phalloidin-Alexa Fluor 555 to label F-actin and DAPI to label DNA. In confocal microcopy images, protrusions were identified as F-actin tails emanating from cells expressing VAMP3-pHluorin into adjacent cells lacking VAMP3-pHluorin. ImageJ software was used to determine FE values for exofacial VAMP3-pHluorin for each protrusion. For detection of recruitment of Exo70, confocal microscopy images of fixed Caco-2 BBE1 cells transiently expressing Exo70-Ha were acquired. The extent of recruitment of Exo70-Ha to protrusions was quantified as FE values, similarly to that as described for FE quantification of exofacial VAMP3-pHluorin.

Quantification of Cell-To-Cell Spread. Spread of *Listeria* in monolayers of Caco-2 BBE1 cells treated with Sec5 siRNA or stably expressing EGFP-Rab11A.S25N or CFP-Rab8A.T22N was performed using focus assays, essentially as described (23–25).

Statistical Analysis. Statistical analysis was performed using Prism (version 7.0; GraphPad Software). In comparisons of data from three or more conditions, analysis of variance was used. The Tukey-Kramer test was used as a posttest. For comparisons of two data sets, Student's *t* test was used. A *P* value of 0.05 or lower was considered significant.

Data Availability. All primary data (i.e., raw images of Western blots and Prism files with quantified data) have been deposited in Zenodo, https://zenodo.org/deposit/3614677 (47).

ACKNOWLEDGMENTS. We thank Maria Carla Parrini for providing the plasmid expressing pcDNA-Exo70-Ha; Sergio Grinstein for the plasmid pSuperEcliptic (SE) mCherry-pHluorin and for initial help with live-imaging experiments; and Laura Gumy, Marcia Goldberg, and Brian Russo for constructive comments on the manuscript. This work was supported by grants from the Marsden Fund of the Royal Society of New Zealand (13-UOO-085), the Health Research Council of New Zealand (17/082), and the University of Otago Research Committee awarded to K.I.

1. K. Ireton, Molecular mechanisms of cell-cell spread of intracellular bacterial pathogens. *Open Biol.* **3**, 130079 (2013).
2. R. L. Lamason, M. D. Welch, Actin-based motility and cell-to-cell spread of bacterial pathogens. *Curr. Opin. Microbiol.* **35**, 48–57 (2017).
3. D. Pantaloni, C. Le Clainche, M. F. Carlier, Mechanism of actin-based motility. *Science* **292**, 1502–1506 (2001).
4. D. M. Monack, J. A. Theriot, Actin-based motility is sufficient for bacterial membrane protrusion formation and host cell uptake. *Cell. Microbiol.* **3**, 633–647 (2001).
5. T. C. Südhof, J. E. Rothman, Membrane fusion: Grappling with SNARE and SM proteins. *Science* **323**, 474–477 (2009).
6. W. Hong, S. Lev, Tethering the assembly of SNARE complexes. *Trends Cell Biol.* **24**, 35–43 (2014).
7. B. Wu, W. Guo, The exocyst at a glance. *J. Cell Sci.* **128**, 2957–2964 (2015).
8. L. Bajno *et al*., Focal exocytosis of VAMP3-containing vesicles at sites of phagosome formation. *J. Cell Biol.* **149**, 697–706 (2000).
9. A. Das, W. Guo, Rabs and the exocyst in ciliogenesis, tubulogenesis and beyond. *Trends Cell Biol.* **21**, 383–386 (2011).
10. M. R. Heider, M. Munson, Exorcising the exocyst complex. *Traffic* **13**, 898–907 (2012).
11. E. Daro, P. van der Sluijs, T. Galli, I. Mellman, Rab4 and cellubrevin define different early endosome populations on the pathway of transferrin receptor recycling. *Proc. Natl. Acad. Sci. U.S.A.* **93**, 9559–9564 (1996).
12. M. Bernabé-Rubio, M. A. Alonso, Routes and machinery of primary cilium biogenesis. *Cell. Mol. Life Sci.* **74**, 4077–4095 (2017).
13. G. Lalli, A. Hall, Ral GTPases regulate neurite branching through GAP-43 and the exocyst complex. *J. Cell Biol.* **171**, 857–869 (2005).
14. K. Hase *et al*., M-Sec promotes membrane nanotube formation by interacting with Ral and the exocyst complex. *Nat. Cell Biol.* **11**, 1427–1432 (2009).
15. C. Schiller *et al*., LST1 promotes the assembly of a molecular machinery responsible for tunneling nanotube formation. *J. Cell Sci.* **126**, 767–777 (2013).
16. K. M. Posfay-Barbe, E. R. Wald, Listeriosis. *Semin. Fetal Neonatal Med.* **14**, 228–233 (2009).
17. K. Jordan, O. McAuliffe, *Listeria monocytogenes* in foods. *Adv. Food Nutr. Res.* **86**, 181–213 (2018).
18. J. A. Vázquez-Boland *et al*., *Listeria* pathogenesis and molecular virulence determinants. *Clin. Microbiol. Rev.* **14**, 584–640 (2001).
19. O. Disson, M. Lecuit, *In vitro* and *in vivo* models to study human listeriosis: Mind the gap. *Microbes Infect.* **15**, 971–980 (2013).
20. M. D. Peterson, M. S. Mooseker, Characterization of the enterocyte-like brush border cytoskeleton of the C2BBe clones of the human intestinal cell line, Caco-2. *J. Cell Sci.* **102**, 581–600 (1992).
21. J. R. Robbins *et al*., *Listeria monocytogenes* exploits normal host cell processes to spread from cell to cell. *J. Cell Biol.* **146**, 1333–1350 (1999).
22. T. Rajabian *et al*., The bacterial virulence factor InlC perturbs apical cell junctions and promotes cell-to-cell spread of *Listeria*. *Nat. Cell Biol.* **11**, 1212–1218 (2009).
23. L. Polle, L. A. Rigano, R. Julian, K. Ireton, W. D. Schubert, Structural details of human tuba recruitment by InlC of *Listeria monocytogenes* elucidate bacterial cell-cell spreading. *Structure* **22**, 304–314 (2014).
24. L. A. Rigano, G. C. Dowd, Y. Wang, K. Ireton, *Listeria monocytogenes* antagonizes the human GTPase Cdc42 to promote bacterial spread. *Cell. Microbiol.* **16**, 1068–1079 (2014).
25. A. Gianfelice *et al*., Host endoplasmic reticulum COPII proteins control cell-to-cell spread of the bacterial pathogen *Listeria monocytogenes*. *Cell. Microbiol.* **17**, 876–892 (2015).
26. F. E. Ortega, E. F. Koslover, J. A. Theriot, *Listeria monocytogenes* cell-to-cell spread in epithelia is heterogeneous and dominated by rare pioneer bacteria. *eLife* **8**, e40032 (2019).
27. G. Miesenböck, D. A. De Angelis, J. E. Rothman, Visualizing secretion and synaptic transmission with pH-sensitive green fluorescent proteins. *Nature* **394**, 192–195 (1998).
28. S. Sankaranarayanan, D. De Angelis, J. E. Rothman, T. A. Ryan, The use of pHluorins for optical measurements of presynaptic activity. *Biophys. J.* **79**, 2199–2208 (2000).
29. R. Frischknecht, A. Fejtova, M. Viesti, A. Stephan, P. Sonderegger, Activity-induced synaptic capture and exocytosis of the neuronal serine protease neurotrypsin. *J. Neurosci.* **28**, 1568–1579 (2008).
30. V. Di Biase *et al*., Surface traffic of dendritic CaV1.2 calcium channels in hippocampal neurons. *J. Neurosci.* **31**, 13682–13694 (2011).
31. T. Liebmann *et al*., A noncanonical postsynaptic transport route for a GPCR belonging to the serotonin receptor family. *J. Neurosci.* **32**, 17998–18008 (2012).
32. D. Jullié, D. Choquet, D. Perrais, Recycling endosomes undergo rapid closure of a fusion pore on exocytosis in neuronal dendrites. *J. Neurosci.* **34**, 11106–11118 (2014).
33. J. D. Wilson, S. A. Shelby, D. Holowka, B. Baird, Rab11 regulates the mast cell exocytic response. *Traffic* **17**, 1027–1041 (2016).
34. C. Huet-Calderwood *et al*., Novel ecto-tagged integrins reveal their trafficking in live cells. *Nat. Commun.* **8**, 570 (2017).
35. J. Riedl *et al*., Lifeact: A versatile marker to visualize F-actin. *Nat. Methods* **5**, 605–607 (2008).
36. H. Nishida-Fukuda, The exocyst: Dynamic machine or static tethering complex? *BioEssays* **41**, e1900056 (2019).
37. D. Leto, A. R. Saltiel, Regulation of glucose transport by insulin: Traffic control of GLUT4. *Nat. Rev. Mol. Cell Biol.* **13**, 383–396 (2012).
38. X. Zuo *et al*., Exo70 interacts with the Arp2/3 complex and regulates cell migration. *Nat. Cell Biol.* **8**, 1383–1388 (2006).
39. J. Liu *et al*., Exo70 stimulates the Arp2/3 complex for lamellipodia formation and directional cell migration. *Curr. Biol.* **22**, 1510–1515 (2012).
40. D. M. Bryant *et al*., A molecular network for *de novo* generation of the apical surface and lumen. *Nat. Cell Biol.* **12**, 1035–1045 (2010).
41. H. Van Ngo, M. Bhalla, D. Y. Chen, K. Ireton, A role for host cell exocytosis in InlB-mediated internalisation of Listeria monocytogenes. *Cell Microbiol.* **19**, e12768 (2017).
42. L. Rauch *et al*., *Staphylococcus aureus* recruits Cdc42GAP through recycling endosomes and the exocyst to invade human endothelial cells. *J. Cell Sci.* **129**, 2937–2949 (2016).
43. P. L. McNeil, T. Kirchhausen, An emergency response team for membrane repair. *Nat. Rev. Mol. Cell Biol.* **6**, 499–505 (2005).
44. M. D. Welch, M. Way, Arp2/3-mediated actin-based motility: A tail of pathogen abuse. *Cell Host Microbe* **14**, 242–255 (2013).
45. J. S. Pearson, C. Giogha, T. Wong Fok Lung, E. L. Hartland, The genetics of enteropathogenic *Escherichia coli* virulence. *Annu. Rev. Genet.* **50**, 493–513 (2016).
46. C. D. Nichols, J. E. Casanova, *Salmonella*-directed recruitment of new membrane to invasion foci via the host exocyst complex. *Curr. Biol.* **20**, 1316–1320 (2010).
47. D. C. Dowd *et al*., Listeria monocytogenes exploits host exocytosis to promote cell-to-cell spread. Zenodo. https://zenodo.org/deposit/3614677. Deposited 24 January 2020.